Neurological Sciences
https://doi.org/10.1007/s10072-020-04611-2

ORIGINAL ARTICLE

Optical coherence tomography angiography findings in Huntington's disease

Laura Giovanna Di Maio[1] · Daniela Montorio[1] · Silvio Peluso[1] · Pasquale Dolce[2] · Elena Salvatore[1] · Giuseppe De Michele[1] · Gilda Cennamo[2]

Received: 22 February 2020 / Accepted: 18 July 2020

Abstract

Objectives To evaluate the retinal and choriocapillaris vascular networks in macular region and the central choroidal thickness (CCT) in patients affected by Huntington disease (HD), using optical coherence tomography angiography (OCTA) and enhanced depth imaging spectral-domain OCT (EDI SD-OCT).

Methods We assessed the vessel density (VD) in superficial capillary plexus (SCP), deep capillary plexus (DCP), and choriocapillaris (CC) using OCTA, while CCT was measured by EDI SD-OCT.

Results Sixteen HD patients (32 eyes) and thirteen healthy controls (26 eyes) were enrolled in this prospective study. No significant difference in retinal and choriocapillaris VD was found between HD patients and controls while CCT turned to be thinner in patients respect to controls. There were no significant relationships between OCTA findings and neurological parameters.

Conclusion The changes in choroidal structure provide useful information regarding the possible neurovascular involvement in the physiopathology of HD. Choroidal vascular network could be a useful parameter to evaluate the vascular impairment that occurs in this neurodegenerative disease.

Keywords Huntington disease · Optical coherence tomography angiography · Vessel density · Central choroidal thickness

Introduction

Huntington disease (HD) is an autosomal dominant neurodegenerative disorder due to an expansion of the cytosine-adenine-guanine (CAG) triplet repeat in the 5′ region of the *HTT* gene. Motor, cognitive, and psychiatric problems characterize the classical clinical phenotype [1].

Until to now, only symptomatic treatments are available for HD, but disease-modifying therapies, based on huntingtin-lowering strategies, are currently experimented in clinical trials [2].

Therefore, biomarkers that can accurately measure disease progression are needed urgently.

Neuroimaging and cerebrospinal fluid markers are now used to track HD development from presymptomatic stages, but they often require invasive procedures or costs and time-consuming processes [3].

Retinal layers have been recently studied to investigate the nervous system out of the striatum in HD patient, using optical coherence tomography (OCT).

OCT is becoming widely available and allows for a non-invasive and rapid examination of the posterior structures of the eye, including the ganglion cell complex (GCC), retinal nerve fiber layer (RNFL), and choroid [4, 5]. Because RNFL axons are unmyelinated, they could represent ideal structures to study the processes of neuro-degeneration, neuro-protection, and even neuro-repair [6].

Previous studies analyzed the structural OCT parameters detecting no changes in peripapillary RNFL average thickness (only in some sectors) and a significant reduction in the macular choroidal thickness in HD patients compared with controls [7, 8].

✉ Daniela Montorio
da.montorio@gmail.com

[1] Department of Neurosciences, Reproductive Sciences and Dentistry, University of Naples Federico II, Via S. Pansini 5, 80133 Naples, Italy

[2] Eye Clinic, Public Health Department, University of Naples Federico II, Naples, Italy

Published online: 22 July 2020

Several evidences showed that the cerebral microvascular changes and blood-brain barrier dysfunction may be involved in HD physiopathology [9, 10].

There are several data supporting the presence of the similar anatomical features between retina and brain therefore to monitor retinal vascular networks using OCT angiography (OCTA), a reliable and non-invasive tool to detect the retinal and choriocapillaris vessel density may be useful to identify biomarkers for the evaluation of pathogenesis and disease progression of HD [11–13].

The primary objective of this study was to evaluate the neurostructural and vascular features of the retina and choroid, using SD-OCT and OCTA, respectively, in patients affected by HD comparing them with a control group.

Moreover, we investigated potential correlations between ophthalmological and neurological parameters in patients affected by HD.

Methods

Sixteen patients (32 eyes) affected by HD were enrolled from October 2017 to July 2018 in the Neurological Clinic of the University of Naples "Federico II."

Thirteen healthy subjects (26 eyes) with a normal ophthalmic examination, no history of intraocular surgery or retinal pathologic features, were included as control group.

Each subject underwent evaluation of best corrected visual acuity (BCVA) according to the Early Treatment of Diabetic Retinopathy Study (ETDRS) [14], slit-lamp biomicroscopy, intraocular pressure measurement, fundus examination with a + 90 D lens, SD-OCT and OCTA.

The central choroidal thickness (CCT) was measured using Spectralis Heidelberg with enhanced depth imaging (EDI) mode (Spectralis, Heidelberg Engineering, Heidelberg, Germany), while the GCC and RNFL thickness were evaluated using Optovue RTVue (software RTVue XR version 2017.1.0.151, Optovue Inc., Fremont, CA, USA).

All patients underwent collection of personal and family history and complete neurological examination.

Exclusion criteria for HD patients and controls included the presence of congenital eye disorders, myopia greater than 6 diopters, history of ocular surgery, the presence of significant lens opacities or any macular disease, previous diagnosis of glaucoma, evidence of vitreoretinal disease, uveitis and diabetic retinopathy, history of other neurological or psychiatric disorders, and low-quality images obtained with OCT.

The study was approved by the Institutional Review Board of the University of Naples Federico II, and all investigations adhered to the tenets of the Declaration of Helsinki. Written informed consents were obtained from the patients enrolled in the study.

Spectral domain optical coherence tomography

The mean circumpapillary RNFL and GCC thickness were evaluated, after pupillary dilation (minimum diameter 5 mm), with SD-OCT (software RTVue XR version 2017.1.0.151, Optovue Inc., Fremont, CA, USA) which captures 26,000 axial scans (A-scans) per second and provides a 5-μm depth resolution in tissue. The optic nerve head map protocol was used to evaluate the circumpapillary RNFL. This protocol generates a circumpapillary RNFL thickness map based on measurements obtained around a circle 3.45 mm in diameter centred on the optic disc. The GCC scan was centred 1-mm temporal to the fovea and covered a square grid (7 mm × 7 mm) on the central macula, and GCC thickness was measured from the internal limiting membrane to the outer boundary of the inner plexiform layer. Two pattern-based diagnostic parameters were also obtained. Focal loss volume was computed as the integral of deviation in areas of significant focal GCC loss divided by the map area. Global loss volume was computed as the sum of negative fractional deviation in the entire area.

Only high-quality images, as defined by a signal strength index above 40, were accepted. The device software generates a significance map with normative database comparison for GCC thickness [15]. An experienced ophthalmologist, blinded to patients' data, performed SD-OCT evaluations. The examiner rejected scans that had motion artifacts, poor centration, incorrect segmentation, or poor focus.

EDI-OCT measurement

The CCT was measured using the Spectralis OCT device in EDI mode (Spectralis, Heidelberg Engineering, Heidelberg, Germany).

It was evaluated in the subfoveal region as a manual linear measurement between the outer border of Bruch's membrane and the most posterior identifiable aspect of the choroidal–scleral interface, which is seen as a hyper-reflective layer in the posterior margin of the choroid in EDI mode. Scans with quality score of less than 20 were excluded from the analysis [16].

Optical coherence tomography angiography

We obtained OCTA images with the Optovue Angiovue System (software RTVue XR version 2017.1.0.151, Optovue Inc., Fremont, CA, USA) which is based on split-spectrum amplitude de-correlation algorithm (SSADA). The instrument has an A-scan rate of 70,000 scans per seconds with a tissue axial resolution of 5 μm and a 15-μm beam width. Each B-scan contained 304 A-scans. Two consecutive B-scans were captured at a fixed position before proceeding to the next sampling location. Blood flowing through vessels

causes a change in reflectance over time and results in localized areas of flow de-correlation between frames. The spectrum of the light source was split into multiple component parts to decrease the noise present in the image; each part was used to perform the de-correlation step, and the results of all the split spectra were averaged. In any given region of tissue, the projection image can be viewed to obtain an image of the contained blood flow [17].

Cross-sectional registered reflectance intensity images and flow images were summarized and viewed as an en face maximum flow projection from the inner limiting layer to the retinal epithelial pigment. Macular capillary network was visualized in scans centred on the fovea by performing a 6 mm × 6 mm scan over the macular region. Vessel density (VD) was defined as the percentage area occupied by the large vessels and microvasculature in the analyzed region [18]. The OCT software, according to the ETDRS classification of diabetic retinopathy, applies to all angiograms a grid centred on fovea, which divides macular region in foveal and parafoveal area. For each eye analyzed, the software automatically calculates vessel density in whole scan area and in all sections of applied grid in different vascular networks of the retina: superficial capillary plexus (SCP) and deep capillary plexus (DCP) and in choriocapillaris (CC). Poor-quality images with a signal strength index less than 40 or registered image sets with residual motion artifacts were excluded from the analysis.

Statistical analysis

We used R Enviroment for statistical computing (http://www.r-project.org) and lme4 to perform a linear mixed effects analysis, to test for differences between patients and controls for each variable measured on both eyes of subjects [19, 20]. As fixed effects, we considered the variable "eye" as well as groups (without interaction term, because it was first tested and found never significant). As random effects, we had intercepts for subjects, to take into account the non-independence that stems from having double measures (right eye and left eye) by the same subject. To test for difference between the two groups in terms of sex and age, we performed Fisher's Exact test and Mann Whitney test, respectively.

Finally, linear mixed effects analysis was also used to investigate potential relationships between ophthalmological and neurological parameters in patients affected by HD, estimating the effect of the following neurological parameters: age at onset of motor symptoms, number of CAG repeats, Total Motor Score-Unified Huntington's Disease Rating Scale, on ophthalmological parameters, considering also the double observations (right eye and left eye) for the ophthalmological parameters on the same patient.

For all statistical analysis, a p value < 0.05 was considered statistically significant.

Results

Sixteen patients (3 females, 13 males, mean age ± SD 57.31 ± 10.22 years) for a total of 32 eyes were included in this prospective study. According to the TFC Total Score, 5 patients were in stage I, 5 in stage II, and 6 in stage III; UHDRS-TMS score was 29.7 ± 12.9; and CAG length was 43.2 ± 3.0. The control group was constituted by 13 healthy subjects (5 females, 8 males, mean age 55.00 ± 11.22 years) for a total of 26 eyes. There were no significant differences for age, sex, and BCVA between patients and controls. The demographic and clinical characteristics of the two cohorts are reported in Table 1.

There were no statistically significant differences between HD patients and controls for SCP, DCP, and CC vessel density, in whole image, parafovea, and fovea (Table 2).

At SD-OCT examination, CCT revealed a significant decrease in patients compared with controls (239.60 ± 59 μm vs 279.46 ± 19.60 μm; $p = 0.0181$), while all GCC and RNFL parameters showed no significant differences between the two groups (Table 3, Fig. 1).

Finally, we analyzed the relationships between the neurological parameters with CCT (the only parameter that was found to be statistically different between patients and controls) in HD patients. We found an inverse correlation between age of onset of motor symptoms and CCT ($\beta = -2.99$, $p = 0.032$), which disappeared after adjusting for age of patients ($\beta = -0.82$, $p = 0.806$).

Similarly, there was no statistically significant relationship between the number of CAG repeats and CCT, after correction for age ($\beta = 10.26$, $p = 0.278$).

Discussion

To our knowledge, this is the first pilot study to evaluate the retinal and choriocapillaris vascular networks using OCTA.

Table 1 Demographic and clinical characteristics in controls and HD patients

	Controls	Patients	p value
Eyes (n)	26	32	
Female/male	5/8	3/13	0.4058
Age (years; mean ± SD)	55.00 ± 11.22	57.31 ± 10.22	0.5736
BCVA (LogMar)	0.05 ± 0.07	0.08 ± 0.11	0.3418

SD standard deviation, *BCVA* best-corrected visual acuity, *logMAR* logarithm of the minimum angle of resolution

BCVA data are expressed as vessel density percentage (mean ± SD)

Fisher's Exact test and Mann Whitney test were used for sex and age and mixed-effects model analysis for BCVA

Table 2 Differences in OCT angiography vessel density between controls and HD patients

	Controls	Patients	*p* value
Superficial capillary plexus (%)			
Whole image	48.17 ± 4.99	48.93 ± 3.28	0.4844
Parafovea	49.58 ± 6.16	50.96 ± 4.32	0.3218
Fovea	24.95 ± 7.22	21.89 ± 8.79	0.2616
Deep capillary plexus (%)			
Whole image	50.52 ± 5.11	48.12 ± 5.44	0.1687
Parafovea	52.69 ± 4.68	52.32 ± 5.33	0.8137
Fovea	36.92 ± 7.85	38.08 ± 10.14	0.7049
Choriocapillaris (%)			
Whole image	71.40 ± 4.40	71.58 ± 4.07	0.8939
Parafovea	71.29 ± 5.29	70.82 ± 3.75	0.7437
Fovea	72.77 ± 6.87	69.65 ± 7.74	0.1396

Data expressed as vessel density percentage (mean ± SD)

p-values obtained by mixed-effects model analysis

In the last three decades, a retinal impairment has been progressively defined in HD. The first studies, identifying electrophysiological changes in a little cohort of HD patients and suggesting an abnormal cone function, have been confirmed by evidences in HD mammalian models [21].

R/6 transgenic mice, a model mimicking juvenile HD, showed first an early and progressive retinal degeneration with significant decrease in the cone nuclei count and a decline in cone-mediated electroretinograms responses [22], and later retinal remodeling processes, Müller cell gliosis, and cell death phenomena [23].

More recently, mutant huntingtin aggregates have been found in all three nuclear layers of R6/2 transgenic mice [24] and seemed selectively affect retinal interneurons [25].

OCT findings in HD appeared variable and conflicting. A significant thinning of temporal peripapillary RNFL, correlated with disease duration, has been observed in the first OCT study in HD patients by Kersten and coworkers; these authors confirmed these data also in a little group of six premanifest HD subjects [7].

In a smaller cohort of HD patients, Andrade et al. have showed no significant differences in peripapillary RNFL thickness or in the different quadrants between patients and controls [8].

More recently, Gatto et al. demonstrated a significant RNFL thinning only in temporal and superior sectors in HD patients compared with controls, similarly to what was noted for other neurodegenerative disorders such as Alzheimer disease and Parkinson disease. It has been hypothesized that the temporal sector is one of the most frequently affected regions in mitochondrial disorders; its involvement in HD could reflect the mitochondrial trafficking impairment [26].

Using single retinal segmentation techniques, thicknesses of the various layers of the retina have been measured in HD patients by Sevim et al. The RNFL thickness in temporal sector, all the inner retinal layers together with the outer plexiform layer appeared reduced in HD patients when compared with controls. Ganglion cell layer has been considered the most affected retinal layer because it is strongly correlated with the progression markers of the disease [27].

Our results demonstrated no statistically significant differences in GCC and RNFL parameters between HD patients and controls as well as no significant changes in retinal and choriocapillaris vessel density in different macular regions.

Regarding the OCTA results, the retinal and choriocapillaris vascular networks did not differ respect to controls, while an interesting result was found in the analysis of the choroidal thickness that turned to be significantly reduced in patients respect to controls.

Table 3 Differences in OCT parameters between controls and HD patients

	Controls	Patients	*p* value
Choroidal thickness (CCT) (μm)	279.46 ± 19.60	239.60 ± 59.00	**0.0181**
Ganglion cell complex (GCC) (μm)			
Average	97.54 ± 5.89	100.83 ± 14.46	0.3333
Superior	97.65 ± 6.41	100.80 ± 16.07	0.4043
Inferior	97.50 ± 5.91	100.87 ± 13.98	0.3110
Global loss volume (GLV)	2.13 ± 2.04	6.39 ± 20.00	0.3016
Focal loss volume (FLV)	0.62 ± 0.64	1.25 ± 2.12	0.2154
Retinal nerve fiber layer (RNFL) (μm)			
Average	101.42 ± 9.12	106.17 ± 13.98	0.2537
Superior	104.12 ± 9.33	110.34 ± 16.39	0.1972
Inferior	98.69 ± 10.28	102.21 ± 13.19	0.3781

Data expressed as vessel density percentage (mean ± SD)

p values obtained by mixed-effects model analysis. Bold *p* values are significant

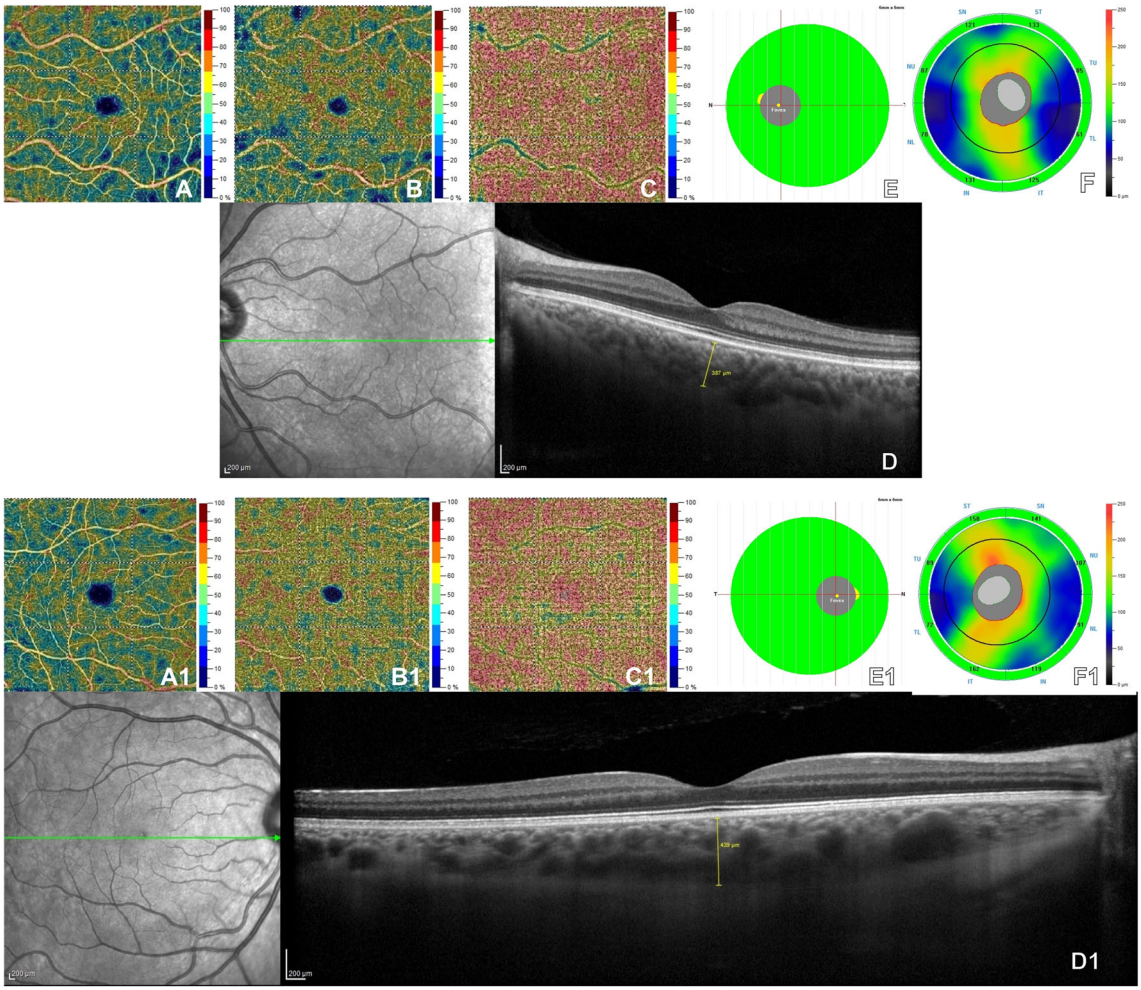

Fig. 1 Optical coherence tomography angiography (OCTA) in the left eye of a HD patient (female, 51 years) showed no alteration in superficial capillary plexus (SCP) (**a**), deep capillary plexus (DCP) (**b**), choriocapillaris (CC) (**c**), and an increase (439 μm) in central choroidal thickness (CCT) (**d**) at enhanced depth imaging spectral-domain OCT (EDI SD-OCT), and a normal thickness in Ganglion Cell Complex (GCC) (**e**) and retinal nerve fiber layer (RNFL) (**f**) at structural OCT. Left eye of healthy control (female, 45 years) showed a normal vascular density in SCP (A1), DCP (B1), CC (C1) at OCTA, a normal CCT (387 μm) (D1) at EDI SD-OCT, and a normal thickness in GCC (E1) and RNFL (F1) at structural OCT.

This parameter did not correlate with UHDRS score, as confirmed also by the study conducted by Andrade et al. that reported a significant reduction in macular choroidal thickness that did not correlate with this motor score [8]. These results could explain, according to these authors, that the choroidal changes could occur earlier than retinal changes.

Several evidences showed that the cerebral neurovascular dysfunction plays a role in the neuronal integrity impairment in HD [9, 10].

The study conducted by Lin et al. found an increased cerebral vessel density in mouse model of HD in the first weeks of age and in human brain tissue sample post-mortem evaluated by functional MRI and immunohistological analysis [9].

These results could be a consequence of a compensatory response to the hypoperfusion [28, 29] that has been evaluated in cerebral tissue (cortex, striatum and basal ganglia) during the neurodegenerative processes occurring in HD [9, 30, 31].

Also the blood-brain barrier (BBB) dysfunction, reported in other studies, could confirm the cerebrovascular impairment as potential implication in pathogenesis of HD [10, 32].

Drouin-Ouellet et al. found a BBB leakage in the striatum of R6/2 mice and in post-mortem human brain tissue; these findings were confirmed by the increase of leukocytes found in the perivascular space of cerebral vessels. This mechanism could allow peripheral blood leukocytes to enter easily the central nervous system inducing the cerebral inflammatory response and, therefore, promoting the neuronal death [10]. Therefore, in our study the decreased CCT could be a consequence of a state of ocular vascular impairment that could be mirror of possible alterations occurring also in the cerebrovascular network contributing to brain atrophy.

In conclusion this study, although presenting as main limitation the small sample size that did not involves the different spectrum of HD, demonstrated the possible involvement of

choroidal vascular impairment in the pathogenesis of HD using OCT. Further longitudinal studies are needed to evaluate a wider study group in order to detect a useful biomarker for the early diagnosis and disease progression of HD.

Author contributions Conceptualization: Giuseppe De Michele, Gilda Cennamo

Methodology: Gilda Cennamo, Daniela Montorio, Laura Giovanna Di Maio

Formal analysis and investigation: Laura Giovanna Di Maio, Daniela Montorio, Pasquale Dolce, Elena Salvatore

Writing—original draft preparation: Daniela Montorio, Silvio Peluso

Writing—review and editing: Daniela Montorio

Supervision: Giuseppe De Michele, Gilda Cennamo.

Compliance with ethical standards

Conflict of interest The authors declare that they have no conflict of interest.

Ethical approval All procedures performed in studies involving human participants were in accordance with the ethical standards of the institutional and/or national research committee and with the 1964 Helsinki Declaration and its later amendments or comparable ethical standards.

Informed consent Informed consent was obtained from all individual participants included in the study002E.

References

1. Walker FO (2007) Huntington's disease. Lancet 369:218–228
2. Tabrizi SJ, Ghosh R, Blair R, Leavitt BR (2019) Huntingtin lowering strategies for disease modification in Huntington's disease. Neuron 101:801–819
3. Zeun P, Scahill RI, Tabrizi SJ, Wild EJ (2019) Fluid and imaging biomarkers for Huntington's disease. Mol Cell Neurosci 97:67–80
4. Huang D, Swanson EA, Lin CP, Schuman JS, Stinson WG, Chang W, Hee M, Flotte T, Gregory K, Puliafito C (1991) Optical coherence tomography. Science 254:1178–1181
5. Mrejen S, Spaide RF (2013) Optical coherence tomography: imaging of the choroid and beyond. Surv Ophthalmol 58:387–429
6. Sakai RE, Feller DJ, Galetta KM, Galetta SL, Balcer LJ (2011) Vision in multiple sclerosis: the story, structure-function correlations, and models for neuroprotection. J Neuroophthalmol 31: 362–373
7. Kersten HM, Danesh-Meyer HV, Kilfoyle DH, Roxburgh RH (2015) Optical coherence tomography findings in Huntington's disease: a potential biomarker of disease progression. J Neurol 262: 2457–2465
8. Andrade C, Beato J, Monteiro A, Costa A, Penas S, Guimarães J (2016) Spectral-domain optical coherence tomography as a potential biomarker in Huntington's disease. Mov Disord 31:377–783
9. Lin CY, Hsu YH, Lin MH, Yang TH, Chen HM, Chen YC, Hsiao HY, Chen CC, Chern Y, Chang C (2013) Neurovascular abnormalities in humans and mice with Huntington's disease. Exp Neurol 250:20–30
10. Drouin-Ouellet J, Sawiak SJ, Cisbani G, Lagacé M, Kuan WL, Saint-Pierre M, Dury RJ, Alata W, St-Amour I, Mason SL, Calon F, Lacroix S, Gowland PA, Francis ST, Barker RA, Cicchetti F (2015) Cerebrovascular and blood-brain barrier impairments in Huntington's disease: potential implications for its pathophysiology. Ann Neurol 78:160–177
11. Patton N, Aslam T, MacGillivray T, Pattie A, Deary IJ, Dhillon B (2005) Retinal vascular image analysis as a potential screening tool for cerebrovascular disease: a rationale based on homology between cerebral and retinal microvasculatures. J Anat 206:319–348
12. London A, Benhar I, Schwartz M (2013) The retina as a window to the brain-from eye research to CNS disorders. Nat Rev Neurol 9: 44–53
13. Wang Q, Chan S, Yang JY, You B, Wang YX, Jonas JB, Wei WB (2016) Vascular density in retina and choriocapillaris as measured by optical coherence tomography angiography. Am J Ophthalmol 168:95–109
14. Kniestedt C, Stamper RL (2003) Visual acuity and its measurement. Ophthalmol Clin N Am 16:155–170
15. Lanzillo R, Cennamo G, Criscuolo C, Carotenuto A, Velotti N, Sparnelli F, Cianflone A, Moccia M, Brescia Morra V (2018) Optical coherence tomography angiography retinal vascular network assessment in multiple sclerosis. Mult Scler 24:1706–1714
16. Spaide RF, Koizumi H, Pozzoni MC, Pozonni MC (2008) Enhanced depth imaging spectral-domain optical coherence tomography. Am J Ophthalmol 146:496–500
17. Jia Y, Tan O, Tokayer J, Potsaid B, Wang Y, Liu JJ, Kraus MF, Subhash H, Fujimoto JG, Hornegger J, Huang D (2012) Split spectrum amplitude-decorrelation angiography with optical coherence tomography. Opt Express 20:4710–4725
18. Huang D, Jia Y, Gao SS, Lumbroso B, Rispoli M (2016) Optical coherence tomography angiography using the optovue device. Dev Ophthalmol 56:6–12
19. Core Team R (2018) R: a language and environment for statistical computing. In: R Foundation for statistical computing. Austria. URL, Vienna https://www.R-project.org/
20. Bates D, Maechler M, Bolker B, Walker S (2015) Fitting linear mixed-effects models using lme4. J Stat Softw 67:1–48
21. Paulus W, Schwarz G, Werner A, Lange H, Bayer A, Hofschuster M, Müller N, Zrenner E (1993) Impairment of retinal increment thresholds in Huntington's disease. Ann Neurol 34(4):574–578
22. Li M, Yasumura D, Ma AA, Matthes MT, Yang H, Nielson G et al (2013) Intravitreal administration of HA-1077, a ROCK inhibitor, improves retinal function in a mouse model of Huntington disease. PLoS One 8:e56026
23. Batcha AH, Greferath U, Jobling AI, Vessey KA, Ward MM, Nithianantharajah J, Hannan AJ, Kalloniatis M, Fletcher EL (2012) Retinal dysfunction, photoreceptor protein dysregulation and neuronal remodelling in the R6/1 mouse model of Huntington's disease. Neurobiol Dis 45:887–896
24. Helmlinger D, Yvert G, Picaud S, Merienne K, Sahel J, Mandel J-L, Devys D (2002) Progressive retinal degeneration and dysfunction in R6 Huntington's disease mice. Hum Mol Genet 11:3351–3359
25. Johnson MA, Gelderblom H, Rüther K, Priller J, Bernstein SL (2014) Evidence that Huntington's disease affects retinal structure and function. Invest Ophthalmol Vis Sci 55:1644
26. Gatto E, Parisi V, Persi G, Rey EF, Cesarini M, Etcheverry JS et al (2018) Optical coherence tomography (OCT) study in Argentinean Huntington's disease patients. Int J Neurosci 128:1157–1162
27. Sevim DG, Unlu M, Gultekin M, Karaca C (2018) Retinal single-layer analysis with optical coherence tomography shows inner retinal layer thinning in Huntington's disease as a potential biomarker. Int Ophthalmol 39:611–621
28. Mironov V, Hritz MA, LaManna JC, Hudetz AG, Harik SI (1994) Architectural alterations in rat cerebral microvessels after hypobaric hypoxia. Brain Res 660:73–80
29. Sekhon LH, Morgan MK, SpenceI (197) Normal perfusion pressure breakthrough: the role of capillaries. J. Neurosurg. 86: 519–524
30. Wolf RC, Gron G, Sambataro F, Vasic N, Wolf ND, Thomann PA et al (2011) Magnetic resonance perfusion imaging of resting-state

cerebral blood flow in preclinical Huntington's disease. J Cereb Blood Flow Metab 31:1908–1918
31. Harris GJ, Codori AM, Lewis RF, Schmidt E, Bedi A, Brandt J (1999) Reduced basal ganglia blood flow and volume in pre-symptomatic, gene-tested persons at-risk for Huntington's disease. Brain 122:1667–1678
32. Duran-Vilaregut J, del Valle J, Manich G, Camins A, Pallas M, Vilaplana J, Pelegri C (2011) Role of matrix metalloproteinase-9 (MMP-9) in striatal blood–brain barrier disruption in a 3-nitropropionic acid model of Huntington's disease. Neuropathol Appl Neurobiol 37:525–537